Journal of Materials Chemistry C

Accepted Manuscript

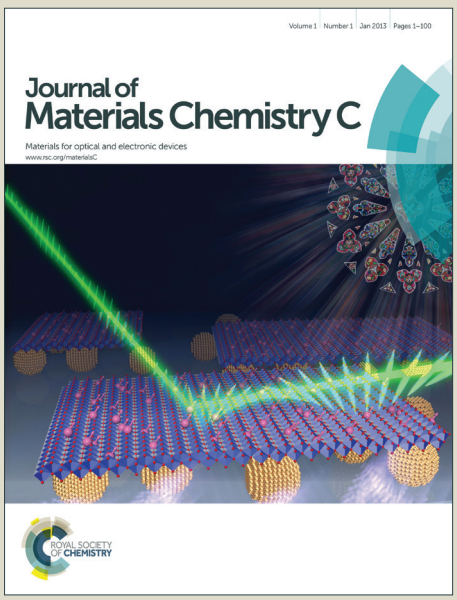

ROYAL SOCIETY OF CHEMISTRY

www.rsc.org/materialsC

Journal of
Materials Chemistry C

RSCPublishing

COMMUNICATION

Robust Anti-Reflective Silica Nanocoatings: the Abrasion Resistance Enhanced via Capillary Condensation of APTES

Cite this: DOI: 10.1039/x0xx00000x

Received 00th **xxxx**, **xxxxx**
Accepted 00th **xxxx**, **xxxxx**

DOI: 10.1039/x0xx00000x

www.rsc.org/

Chao Cai,[†ab] Xiaoli Yang,[†ab] Zhen Wang,[ab] Haixia Dong,[a] Hongwei Ma,[c] Ning Zhao*[a] and Jian Xu*[a]

This paper demonstrates a facile and effective improvement of abrasion resistance of silica nanoparticles (NPs) based anti-reflective coatings via capillary condensation of 3-aminopropyl triethoxysilane (APTES). Quartz crystal microbalance (QCM) is used to test the abrasion resistance property. The versatility of this developed method is further illustrated by a successful application to the poor heat-resistant polymer substrates.

Solar energy, as a clean and inexhaustible resource, has shown promising prospect in replacing traditional energy sources. One of the devices to convert solar energy into electricity is the solar cells. However, adoption of solar cells is still limited because of its inefficiency in photoelectric conversion and the high cost.[1] Therefore, improving the photoelectric conversion efficiency of the solar cells is in high demand. One of the potential solutions is to coat the cover glass of the solar panel with anti-reflective (AR) coating, which can decrease light reflection and allowing more photons to enter the conversion region [2-6] AR coatings are also indispensable in panel displays, light emitting diodes (LEDs) and other optical devices, for the purpose of decreasing reflection and increasing transmittance of incident light.[7-10] Inspired from the corneal of moths, almost perfect antireflection can be achieved depending on the periodic nanostructure. Many analogous structures have been fabricated via top-down methods, such as nanoimprint lithography[11], colloidal lithography,[12, 13] direct replication[5, 14], physical etching[15, 16]and chemical etching[17, 18]. However, these methods meet their main limitations, such as the lack of versatility and significant cost, when applied at a large scale in practice. For this reason, AR coatings, fabricated with bottom-up methods, especially silica NPs based AR coatings have been highly sought after[19-22], given that silica NPs possess prominent AR property, low cost, capability of large-scale production and relatively excellent universality for substrates. For different user requirements, AR coatings have been endowed all kinds of functionalities, such as anti-fogging[23], self-cleaning [24-27]and intelligence[28]. In addition to these extra functionalities, mechanical durability, concerning the service life of the nanocoatings, is fundamental in practice.

To improve the mechanical stability of the silica-based nano-porous coatings, numerous strategies have been explored, among which high-temperature sintering[29, 30] is the most common approach. However, this approach is only applicable to heat-resistant substrate like glass. As for polymer substrates with poor heat-resistance, this method is impractical[31]. Tan et al.[32] recently utilized a new technology "sink and etch" to fabricate a template inverse porous surface on the PMMA substrate, showing superior mechanical stability. Still and all, developing other more universal methods operated at moderate temperature, would impulse practical applications of AR coatings in more wide-ranging areas[33]. Atomic layer deposition[34, 35] and hydrothermal method[36] have also been developed to improve mechanical robustness of the nanocoatings. However these methods require multi-step operations, costly instruments, or specific surface chemistry and are therefore less practical in large scale applications.

Capillary condensation, although undesired in nanomaterials, is an effective functionalization approach for NPs formed films, in which functional agent can be brought in by an isothermal vapor-

[a] *Beijing National Laboratory for Molecular Sciences, Laboratory of Polymer Physics and Chemistry, Institute of Chemistry, Chinese Academy of Sciences, Beijing 100190, People's Republic of China.*
[b] *University of Chinese Academy of Sciences, Beijing 100049, People's Republic of China.*
[c] *Suzhou Institute of Nano-Tech and Nano-Bionics, Chinese Academy of Sciences, Suzhou, 215123, People's Republic of China.*
[†] These authors contributed equally.

condensation process[37]. Capillary condensation is particle-size-dependent. The smaller the particles, the more volume of the voids between them tend to be filled by the functional agent[38]. Thus, silica NPs based coatings should be more sensitive to capillary condensation. By rationally selecting the functional agent, it is expected to improve the corresponding properties as needed. Herein, we utilized APTES as an adhesive agent to improve the durability of silica-based AR coatings. By carefully control of the deposition conditions, capillary condensation would be obtained and the mechanical durability would be improved without sacrificing the AR property. In the atmosphere of moisture and NH_3, siloxane molecules would hydrolyze into condensed siloxane[39]. Thus, the deposition of the vapor is accompanied by simultaneous chemical reaction of APTES, which would make a strong connection between silica particles. QCM is used to quantitatively test the abrasion resistance property of the AR coatings. Benefiting from the moderate operation temperature and the facile procedure, this method can be applied to polymeric substrate, which has poor heat-resistance.

During the capillary condensation process, APTES firstly evaporated from the vial and then the vapor would be absorbed into the voids of SiO_2 NPs film due to the hydrodynamic driving force.[38,40] Meanwhile, intermolecular self-condensation and condensation with Si-OH groups on the SiO_2 NPs would occur as water and NH_3 exist. In this case, chemical bonding makes NPs adhere to each other strongly and capillary condensation brings none-destruction to the original surface morphology and the porous structure, which is critical to maintain the AR property.

Generally, the AR films should be assembled with NPs of sub-100 nm to avoid Rayleigh scattering. However, in order to intuitively demonstrate the adhesion of the particles through capillary condensation, 100-nm SiO_2 NPs was used as a model system here. After the spin-coating process, a flat NPs-formed coating was obtained. The original coating is composed of boundary-smooth SiO_2 particles that stack close, yet without obvious interparticle junctions (Fig. 1A), imply a relatively fragile property. The profile view clearly shows a poor adhering of the SiO_2 particles to the substrate (Fig. 1C). After capillary condensation with APTES for 2 h, the stacked particles are turned into one conjoined structure, with capillary bridging between the SiO_2 particles (Fig. 1B and D). Once the duration of capillary condensation were to last longer (Fig. S1) or a film-wise condensation were to occur, the surface would be covered by a several-micrometer thick deposits layer, burying the NPs and leaving no porous structure. In the case of capillary condensation (Fig. 1B), the shape of the particles can still be distinguishable compared with Fig. 1A. Beyond that, condensed APTES provides a transitional layer between the substrate and the particles, which secures the fastness of the coating (Fig. 1D). The two factors - the retained porous structure from the capillary condensation and the strong interparticle bonding from chemical condensation of APTES -are the keys to achieve both an excellent AR property and the mechanical robustness.

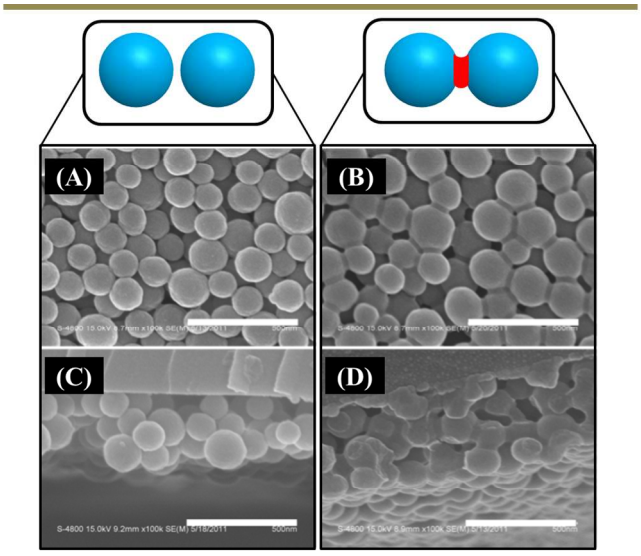

Fig. 1 SEM images shown morphology comparison of SiO_2 NPs films before (the left column) and after (the right column) capillary condensation of APTES. (The capillary condensation process lasts for 2 h) (A) and (B) show the top views while (C) and (D) are the profile images. The schematic diagrams on top of the SEM images illustrate the interparticle bonding state in the corresponding situations. All the scale bars in the SEM images are 500 nm.

Theoretically, in an isothermal process, capillary condensation occurs regardless of the chemistry of the particles or the vapors[23]. A successful capillary condensation is the foundation of the final target. In consequence, given the AR property, for coatings composed of sub-100-nm particles (Fig. S2), several measurements instead of SEM were carried out to prove the reliability of this method. 30-nm SiO_2 NPs were utilized to construct the AR coatings. A film-wise condensation, which may result from losing control of a constant temperature, should be avoided in order to achieve an excellent AR property. Once the film-wise condensation were to occur, the morphology and thickness of the coatings would be drastically altered, leading to a failure in the anti-reflection. Thus, the surface roughness and the film thickness would not change notably when capillary condensation occurs whereas the refractive index does change accordingly. Based on this criterion, whether a capillary condensation will occur or not can be predicted.

The roughness of the nanoparticle-based AR coatings, obtained from AFM characterizations, shows slight increase with condensation of APTES (Table 1, Fig. S3). The increase of R_a and R_q values may result from even smaller particles formation during the process of APTES condensing.

Table 1 Surface roughness of the coatings calculated from AFM images for original and different APTES-treated samples.

	Original	1 h	2 h	4 h	7 h
R_a (nm)	2.22	3.14	3.05	3.57	3.84
R_q (nm)	2.79	3.99	3.87	4.53	4.81

R_a: Arithmetic average of the absolute values of the height

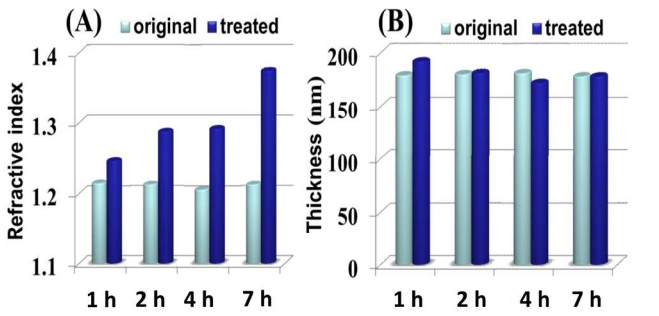

Fig. 2 Deviations of refractive index (A) and film thickness (B) of the AR coatings detected by ellipsometer. The deviation trends prove the occurrence of capillary condensation.

deviations.
R_q: Root mean square average of the height deviations.

The deviations of the refractive index (RI) and film thickness are other proofs of a capillary condensation. RI of the pristine coatings is around 1.2. After APTES condensation, the RI values increase by 0.031, 0.075, 0.086 and 0.162 for samples that have been treated for 1 h, 2 h, 4 h and 7 h, respectively (Fig. 2A). With the increase of the treatment durations, more APTES fill into the voids of the coatings, leading to a decrease in porosity and an increase of the RI values. An appropriate porosity is important for adjusting RI of the AR coating to an ideal value, around 1.23 for a glass substrate (generally with a RI of 1.5).[41] It is vital and fundamental to maintain a proper porosity for any strategy trying to improve the comprehensive properties of the AR coatings. At the same time, the film thicknesses after different treatment durations shows negligible changes (Fig. 2B), which excludes the possibility of a several-micrometre layer formation by film-wise condensation. In conclusion, a capillary condensation of APTES in the NPs based film is achieved.

The transmittance of the APTES-treated films shows slight improvement, comparing the original ones with 1-hour and 2-hour treatment samples (Fig. 3A and B). As aforementioned, the ideal RI, 1.23, is necessary for a perfect AR property in theory. After APTES treatment, RI increases from 1.2 to 1.23, in the case of 1-hour APTES treatment. Therefore, the condensation of APTES into the voids makes a more proper porosity, resulting in an improvement in AR property. However, extensive treatment would make the transmittance of the AR films decline notably, especially in the range of 400-600 nm (Fig. 3C and D). This also agrees with the results of RI test: a further increase of the RI, as a result of reduction of porosity, leads to a decrease of transmittance. Therefore, the treatment time should be kept below 2 h in order to maintain a qualified transmittance.

The capillary condensation process provides a strong covalent bond both internally and interfacially, which would endow the AR coatings robust mechanical durability. Here, the abrasion resistance was quantitatively estimated by a weighing method. QCM was utilized to estimate the abrasion proof of the AR coatings. QCM, as a sensitive device for the mass changes of the chip, can detect mass changes in nanogram·cm^{-2} scale based on Sauerbrey equation, which shows the proportional relevance between the mass change (Δm) and the frequency shift (Δf). Equation (1) is the simplified form of Sauerbrey equation: the constant C=17.7 ng/ (cm^2 Hz) which is dependent on the AT-cut quartz crystal with a fundamental resonant of 5 MHz and the overtone number n (n=1, 3, 5…). The mass change can be calculated by detecting the frequency shift on the chip.

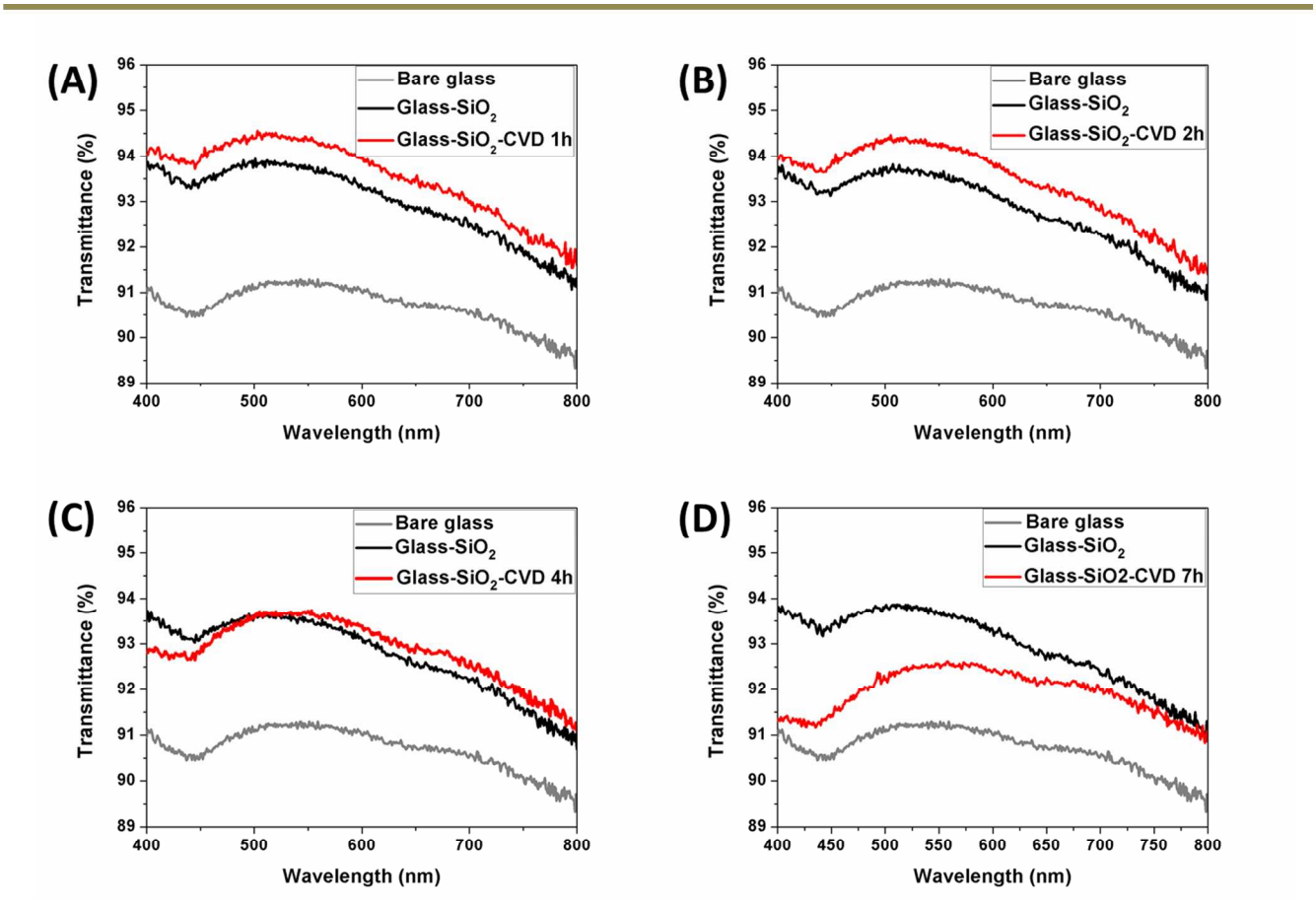

Fig. 3 The AR property of SiO_2 NPs coatings on the glass substrate with APTES treatment. The samples are treated with different durations: (A) 1 h, (B) 2 h, (C) 4 h and (D) 7 h.

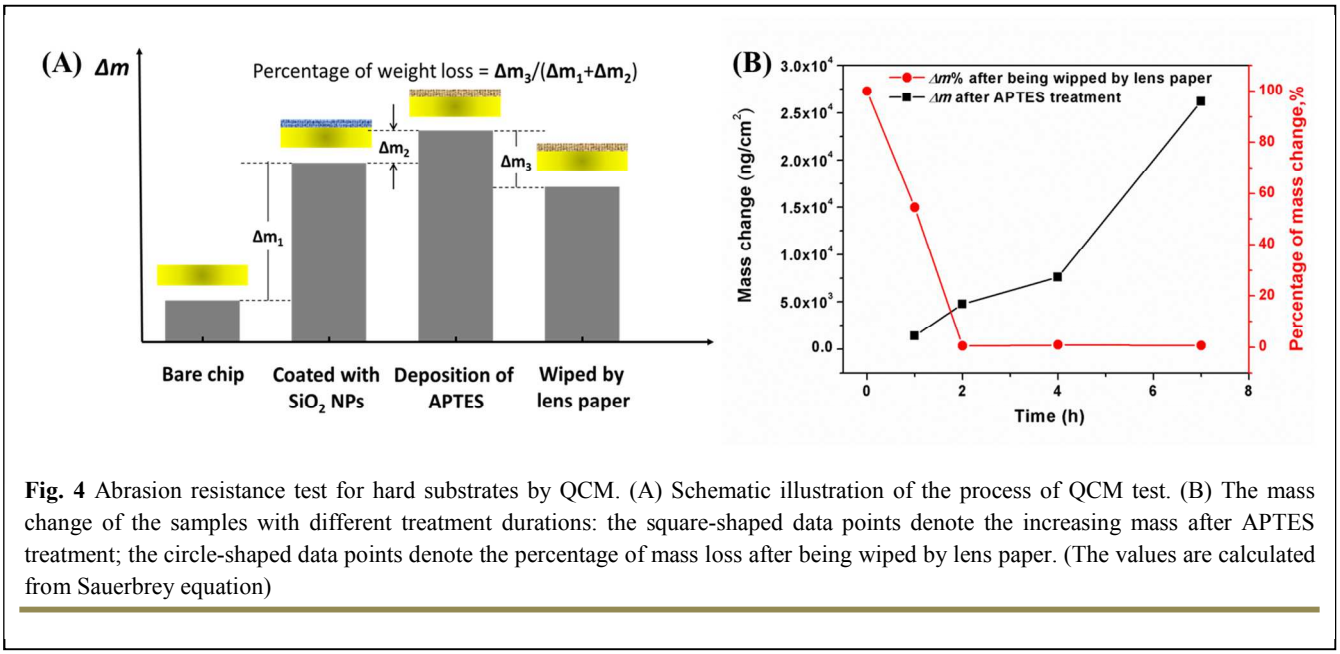

Fig. 4 Abrasion resistance test for hard substrates by QCM. (A) Schematic illustration of the process of QCM test. (B) The mass change of the samples with different treatment durations: the square-shaped data points denote the increasing mass after APTES treatment; the circle-shaped data points denote the percentage of mass loss after being wiped by lens paper. (The values are calculated from Sauerbrey equation)

$$\Delta m = -C \cdot \Delta f / n \quad (1)$$

Table 2 Summary of recorded mass changes of the quartz chip, Δm_1, Δm_2 and Δm_3, during the abrasion resistance test.

	Reference Sample	1 h	2 h	4 h	7 h
Δm_1(μg/cm^2)	18.78	18.68	18.00	18.31	17.27
Δm_2(μg/cm^2)	-	1.38	4.75	7.60	26.19
Δm_3(μg/cm^2)	-18.78	-10.96	-0.12	-0.25	-0.31

The whole QCM test process was conducted as illustrated in Fig. 4A. In our experiment, 4 fundamental frequency values of the chips were recorded and 3 frequency shift values (in proportion for Δm_1, Δm_2, and Δm_3 respectively) were obtained. The calculated deviations of mass are listed in Table 2. Δm_1 denotes the mass of AR coating spin-coated on the chip and the results shows a good reproducibility (all around 18 μg/cm^2). After different durations of APTES treatment, the mass change values, Δm_2, increased with treatment time (Fig. 4 B).Then, all samples were wiped by lens paper for five times and the mass change during this operation was recorded as Δm_3. For the control sample without APTES treatment, almost all particles were peeled off according to its value of Δm_3. With APTES treatment, an obvious improvement in abrasion proof can be seen, especially, the APTES treatment beyond 2 h would make so strong bonding that Δm_3 revealed almost no decrease. For the 7 h treatment sample, capillary condensation brings mass increase by 26.19 μg/cm^2, which is even more than the mass of SiO_2 NPs spin-coated on the chip (17.27 μg/cm^2), indicating a drastically decrease of the porosity of the coating. This further demonstrates why RI increases and transmittance decreases for an excess APTES treatment. As shown in Fig. 4B, beyond 2 h treatment, the coating shows effective abrasion resistance. The quantitative mass changes in QCM test provide a convincing proof of the reinforced abrasion

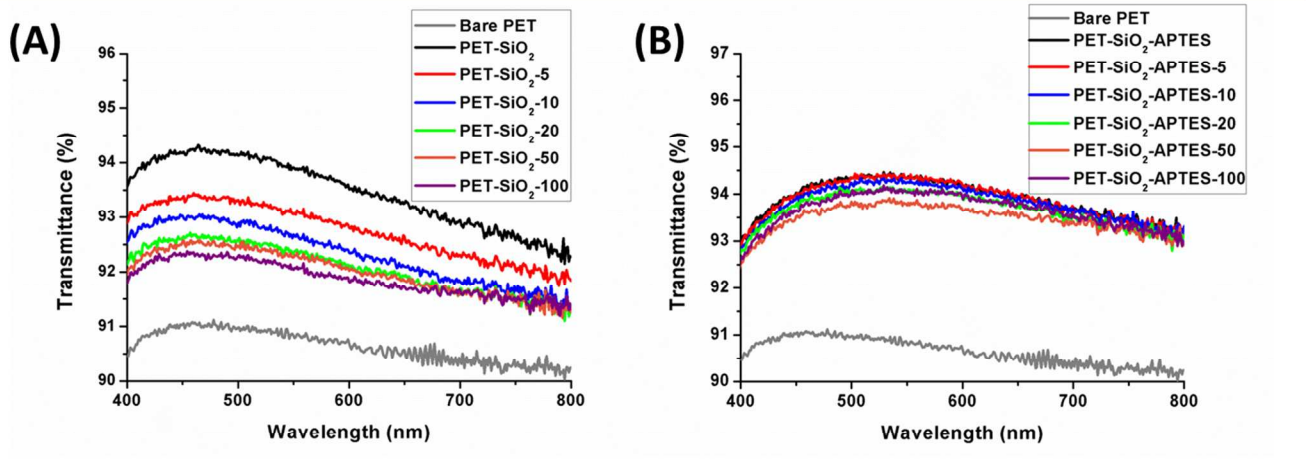

Fig 5 Abrasion resistance for polymer (PET) substrate determined by the transmittance changes: (A) the samples without APTES treatment; (B) the samples with APTES treatment. The numbers in the legend denote the times of wiping performed.

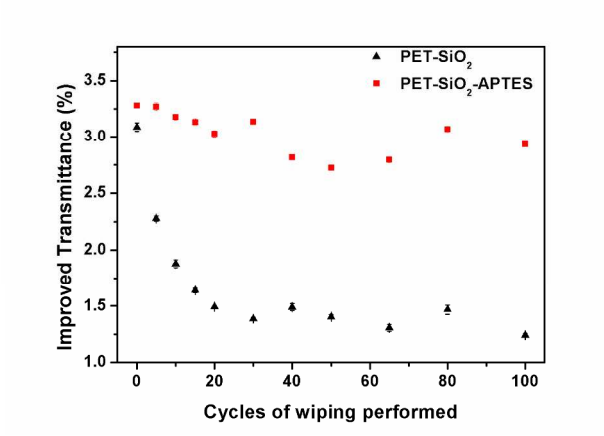

Fig. 6 The net increased transmittance (the transmittance of bare PET is deducted) variations at a specific wavelength (500 nm) based on the curves in Fig. 5.

resistance. QCM test has demonstrated its application as a novel characterization method for quantitative comparison of abrasion resistance property, where only small amount of samples is needed but the resolution is high.

Because of the moderate operation temperature, this method is suitable for polymer substrate. Unlike traditional sintering pathway, the mechanical stability can be improved at a temperature that is harmless to the polymer substrate. To demonstrate the universality of this method, we applied the same operations that were applied to hard substrate to AR coatings on PET substrate. After APTES treatments for 2 h, the samples were wiped repeatedly with lens paper and the transmittance was recorded as a function of the number of wiping performed. In this case, the durability of the coatings would be reflected by the transmittance variations. As illustrated in Fig. 5A, the AR coating without APTES treatment shows a notable decrease in transmittance with the increase of cycles of wiping performed, which strongly indicated the poor abrasion resistance against shear forces. After the initial 5 times of wiping performed, the original SiO_2 NPs formed structure has already shown a drastic drop in transmittance. With APTES treatment, the AR property is maintained when the sample is subjected to on-going wiping (Fig. 5 B). Continued wiping leads to a further but slow transmittance decrease. Fig. 6 demonstrated a more quantitative result, where the improved transmittance values at 500 nm are summarized. The net increased transmittance for the samples without APTES treatment drops from the initial 3.1% to 1.2% after 100 cycles of wiping (triangle-shaped data points, Fig. 6). While that of the samples with APTES treatment shows only slight drop in transmittance (square-shaped data points, Fig. 6). Even after the sample was wiped for 100 times, the net increased transmittance still keeps at around 3.0%. Therefore, the aforementioned results indicate a strong improvement in mechanical durability after APTES treatment

Conclusions

In summary, the abrasion resistance of silica AR nanocoatings has been notably improved by capillary condensation under moderate condition. Due to the capillary condensation, the deposited APTES forms interparticle capillary bridges while the original porous morphology is largely maintained. Meanwhile, the condensation of APTES resulted in covalent bonding between the particles which strongly improves the mechanical stability of the coatings. By controlling the APTES treatment time, an optimal combination of abrasion resistance and AR properties can be achieved. QCM is utilized to evaluate the abrasion resistance property of the AR nanocoatings for the first time. The most remarkable contribution of this method lies in the successful application on polymeric substrate which has poor heat-resistance. This method offers a promising way to improve the AR property and abrasion resistance of screen protection films for electronics, like cellphones, tablet PC and so forth. This method can also be applied to other siloxanes with various functional groups for functionalization of AR coatings, expanding the application areas of the silica NPs based coatings.

Acknowledgments

The authors are grateful for the financial support from the Ministry of Science and Technology (2012CB933800, 2013CB933000) and the National Natural Science Foundation of China (21421061).

Notes and references

1. H. P. Wang, D. H. Lien, M. L. Tsai, C. A. Lin, H. C. Chang, K. Y. Lai and J. H. He, *Journal of Materials Chemistry C*, 2014, **2**, 3144-3171.
2. R. Li, J. T. Di, Z. Z. Yong, B. Q. Sun and Q. W. Li, *Journal of Materials Chemistry A*, 2014, **2**, 4140-4143.
3. Y. A. Dai, H. C. Chang, K. Y. Lai, C. A. Lin, R. J. Chung, G. R. Lin and J. H. He, *Journal of Materials Chemistry*, 2010, **20**, 10924-10930.
4. Y. J. Lee, D. S. Ruby, D. W. Peters, B. B. McKenzie and J. W. P. Hsu, *Nano Letters*, 2008, **8**, 1501-1505.
5. X. Y. Zhang, D. Y. Ji, T. Lei, B. Zhao, K. Song, W. P. Hu, J. Y. Wang, J. Pei and Y. P. Wang, *Journal of Materials Chemistry A*, 2013, **1**, 10607-10611.
6. S. Jeong, E. C. Garnett, S. Wang, Z. G. Yu, S. H. Fan, M. L. Brongersma, M. D. McGehee and Y. Cui, *Nano Letters*, 2012, **12**, 2971-2976.
7. B. Daglar, T. Khudiyev, G. B. Demirel, F. Buyukserin and M. Bayindir, *Journal of Materials Chemistry C*, 2013, **1**, 7842-7848.
8. Y. Li, J. Zhang and B. Yang, *Nano Today*, 2010, **5**, 117-127.
9. J. A. Hiller, J. D. Mendelsohn and M. F. Rubner, *Nat Mater*, 2002, **1**, 59-63.
10. K. Forberich, G. Dennler, M. C. Scharber, K. Hingerl, T. Fromherz and C. J. Brabec, *Thin Solid Films*, 2008, **516**, 7167-7170.
11. S.-J. Choi and S.-Y. Huh, *Macromolecular Rapid Communications*, 2010, **31**, 539-544.
12. Y. Li, J. Zhang, S. Zhu, H. Dong, F. Jia, Z. Wang, Z. Sun, L. Zhang, Y. Li, H. Li, W. Xu and B. Yang, *Adv. Mater.*, 2009, **21**, 4731-4734.
13. L. Li, T. Y. Zhai, H. B. Zeng, X. S. Fang, Y. Bando and D. Golberg, *Journal of Materials Chemistry*, 2011, **21**, 40-56.
14. D.-H. Ko, J. R. Tumbleston, K. J. Henderson, L. E. Euliss, J. M. DeSimone, R. Lopez and E. T. Samulski, *Soft Matter*, 2011, **7**, 6404-6407.
15. C. H. Lin, J. Shieh, C. C. Liang, C. C. Cheng and Y. C. Chen, *Journal of Materials Chemistry C*, 2014, **2**, 3645-3650.

16. Y.-F. Huang, S. Chattopadhyay, Y.-J. Jen, C.-Y. Peng, T.-A. Liu, Y.-K. Hsu, C.-L. Pan, H.-C. Lo, C.-H. Hsu, Y.-H. Chang, C.-S. Lee, K.-H. Chen and L.-C. Chen, *Nat Nano*, 2007, **2**, 770-774.
17. Y. C. Chen, P. Y. Su, S. C. Tseng, Y. C. Lee and H. L. Chen, *Journal of Materials Chemistry A*, 2014, **2**, 4633-4641.
18. D. Qi, N. Lu, H. Xu, B. Yang, C. Huang, M. Xu, L. Gao, Z. Wang and L. Chi, *Langmuir*, 2009, **25**, 7769-7772.
19. A. Yildirim, T. Khudiyev, B. Daglar, H. Budunoglu, A. K. Okyay and M. Bayindir, *ACS Applied Materials & Interfaces*, 2013, **5**, 853-860.
20. Y. Hoshikawa, H. Yabe, A. Nomura, T. Yamaki, A. Shimojima and T. Okubo, *Chemistry of Materials*, 2009, **22**, 12-14.
21. M. Faustini, L. Nicole, C. Boissière, P. Innocenzi, C. Sanchez and D. Grosso, *Chemistry of Materials*, 2010, **22**, 4406-4413.
22. L. Xu and J. He, *Journal of Materials Chemistry C*, 2013, **1**, 4655-4662.
23. D. Lee, M. F. Rubner and R. E. Cohen, *Nano Letters*, 2006, **6**, 2305-2312.
24. P. Ragesh, V. Anand Ganesh, S. V. Nair and A. S. Nair, *Journal of Materials Chemistry A*, 2014, **2**, 14773-14797.
25. J. Bravo, L. Zhai, Z. Wu, R. E. Cohen and M. F. Rubner, *Langmuir*, 2007, **23**, 7293-7298.
26. X.-T. Zhang, O. Sato, M. Taguchi, Y. Einaga, T. Murakami and A. Fujishima, *Chemistry of Materials*, 2005, **17**, 696-700.
27. L. Yao and J. He, *Journal of Materials Chemistry A*, 2014, **2**, 6994-7003.
28. J. Han, Y. Dou, M. Wei, D. G. Evans and X. Duan, *Angewandte Chemie-International Edition*, 2010, **49**, 2171-2174.
29. L. Xu, J. He and L. Yao, *Journal of Materials Chemistry A*, 2014, **2**, 402-409.
30. H. Shimomura, Z. Gemici, R. E. Cohen and M. F. Rubner, *ACS Applied Materials & Interfaces*, 2010, **2**, 813-820.
31. B. Latella, G. Triani, Z. Zhang, K. Short, J. Bartlett and M. Ignat, *Thin Solid Films*, 2007, **515**, 3138-3145.
32. W. S. Tan, Y. Du, L. E. Luna, Y. Khitass, R. E. Cohen and M. F. Rubner, *Langmuir*, 2012, **28**, 13496-13502.
33. J. H. Rouse, B. A. MacNeill and G. S. Ferguson, *Chemistry of Materials*, 2000, **12**, 2502-2507.
34. Liang, S. M. George, A. W. Weimer, N.-H. Li, J. H. Blackson, J. D. Harris and P. Li, *Chemistry of Materials*, 2007, **19**, 5388-5394.
35. M. I. Dafinone, G. Feng, T. Brugarolas, K. E. Tettey and D. Lee, *Acs Nano*, 2011, **5**, 5078-5087.
36. Z. Gemici, H. Shimomura, R. E. Cohen and M. F. Rubner, *Langmuir*, 2008, **24**, 2168-2177.
37. S. Kim and S. H. Ehrman, *Langmuir*, 2007, **23**, 2497-2504.
38. Z. Gemici, P. I. Schwachulla, E. H. Williamson, M. F. Rubner and R. E. Cohen, *Nano letters*, 2009, **9**, 1064-1070.
39. Z. Geng and J. He, *Journal of Materials Chemistry A*, 2014, **2**, 16601-16607.
40. S. Leroch and M. Wendland, *Langmuir*, 2013, **29**, 12410-12420.
41. X. Lu, Z. Wang, X. Yang, X. Xu, L. Zhang, N. Zhao and J. Xu, *Surface and Coatings Technology*, 2011, **206**, 1490-1494.

Capillary condensation of APTES into silica anti-reflective coatings offers both excellent anti-reflective property and robust mechanical durability.